

Cold Denaturation-Induced Conformational Changes in Phosphoglycerate Kinase from Yeast[†]

Gregor Damaschun, Hilde Damaschun, Klaus Gast, Rolf Misselwitz, Jürgen J. Müller, Wolfgang Pfeil, and Dietrich Zirwer*

Max Delbrück Center for Molecular Medicine, Robert-Rössle-Strasse 10, 13125 Berlin-Buch, Germany

Received March 10, 1993; Revised Manuscript Received April 26, 1993

ABSTRACT: The temperature-dependent conformational equilibrium of 3-phosphoglycerate kinase has been studied in the temperature range from 1 to 30 °C by means of dynamic light scattering, small-angle X-ray scattering, differential scanning calorimetry, circular dichroism spectroscopy, and fluorescence spectroscopy. At 28 °C and in the presence of 0.7 M guanidine hydrochloride (GuHCl), the radius of gyration (R_G) and the Stokes radius (R_S) are 2.44 and 3.09 nm, respectively. Decreasing the temperature effects unfolding of the molecule, a process that involves two stages. The two stages correspond to the successive unfolding of the N-terminal and C-terminal domains. The peak maxima of the excess heat capacity, determined from differential calorimetric scans, extrapolated to 0 scan rate, are positioned at 16.5 °C for the N-terminal domain and at 6.3 °C for the C-terminal domain. At 4.5 °C, the radius of gyration and the Stokes radius increase to 7.8 and 4.8 nm, respectively. The persistence length and the length of the statistical chain segment of the unfolded polypeptide chain are 1.74 and 3.48 nm, corresponding to five and ten amino acids, respectively. At 1 °C, the dimensions of the unfolded chain nearly agree with the predicted dimensions under θ conditions. Thus, the conformational changes upon cold denaturation can be described by a transition from a compactly folded molecule to a random coil. The conformation-dependent ratio $\rho = R_G R_S^{-1}$ increases from $\rho = 0.79$ to $\rho = 1.63$. The volume of the unfolded chain is 30 times larger than that of the folded chain in the native state. The unfolding/refolding processes of PGK in the GuHCl-containing solvent are governed by slow kinetics. Thermodynamic equilibrium is reached only some hours after the temperature is changed.

The conformational characterization of unfolded states of proteins is very important in connection with the protein folding problem, because the unfolded state is the starting point in the folding pathway from the “denatured” to the “native” conformation. *In vitro* refolding studies may provide insight into particulars of the folding pathway (e.g., the occurrence of transient intermediates), as suggested by a number of studies (Jaenicke, 1987; Dill & Shortle, 1991). However, a complete understanding of the folding mechanism requires precise knowledge of the protein conformation in the denatured state, since the conformation may vary considerably depending on the applied denaturing procedure, e.g., heating, extreme pH values, or addition of strong denaturants such as urea or GuHCl¹ (Tanford, 1968; Jaenicke, 1987; Damaschun et al., 1991a; Gast et al. 1992a; Sosnick & Trewhella, 1992).

Cold denaturation of globular proteins in aqueous solvents has attracted much attention in the past years. It has been known for some time that the native structure of globular proteins may be unfolded not only by heat denaturation but also by decreasing temperature, i.e., by cold denaturation (Brandts, 1964; Pace & Tanford, 1968; Nojima et al., 1977).

Recently, the theoretical foundation of this phenomenon has been derived from the thermodynamics of protein

denaturation (Privalov & Gill, 1988; Privalov, 1990). Further experimental work has provided increased evidence of the prevalence of cold denaturation in globular proteins (Privalov, 1989; Chen & Schellman, 1989; Chen et al., 1989; Antonino et al., 1991; Tamura et al., 1991a,b; Azuaga et al., 1992; Kuroda et al., 1992). The preferred experimental techniques in these studies are DSC and spectroscopic methods such as CD, fluorescence, and NMR. However, little is known about geometric structural parameters of cold-denatured proteins. It is of great interest to investigate whether cold-denatured proteins have an unfolded structure like a Gaussian coil (Damaschun et al., 1991a,b; Bohdanecky & Petrus, 1991) or the conformation of compact, denatured proteins like the so-called “molten globule state” (Kuwajima 1989; Ptitsyn, 1987; Damaschun et al., 1986). We have found for heat-denatured proteins that the dimensions of the denatured polymer chain are smaller than those of the coil in the θ -state (Gast et al., 1992a), in contrast to acid-denatured proteins at low ionic strength and proteins unfolded by GuHCl (Damaschun et al., 1991a).

We have studied this question using the enzyme 3-phosphoglycerate kinase (PGK) from yeast. The structural and physicochemical properties of this single-chain protein are well-known. PGK consists of 415 amino acids, which are organized in two widely separated domains of about equal size connected by a hinge (Banks et al., 1979; Watson et al., 1982; Harlos et al., 1992). Yeast PGK contains two tryptophans, and both are in the C-terminal domain. The protein lacks disulfide bridges. Thermal denaturation of yeast PGK has been studied by Hu and Sturtevant (1987) and Galisteo et al. (1991) by means of DSC. Only one denaturation peak was observed under all conditions. However, irreversibility of thermal unfolding was clearly indicated.

[†] Supported by grants from the Deutsche Forschungsgemeinschaft (Da 292/1-1 and Pf 252/1-1) and the Bundesministerium für Forschung und Technologie (0319682 A) and by a grant from the Fonds der chemischen Industrie to G.D.

¹ Abbreviations: CD, circular dichroism; DLS, dynamic light scattering; DSC, differential scanning calorimetry; DTT, dithiothreitol; EDTA, ethylenediaminetetraacetic acid; GuHCl, guanidine hydrochloride; FT-DSC, Fourier transform differential scanning calorimetry; PGK, 3-phosphoglycerate kinase (EC 2.7.2.3); SAXS, small-angle X-ray scattering; WAXS, wide-angle X-ray scattering.

Cold denaturation as well as heat denaturation of yeast PGK under mildly destabilizing conditions, i.e., in the presence of 0.7 M GuHCl, has been investigated by Griko et al. (1989) using DSC, CD, and fluorescence. Interestingly, they found that cold denaturation proceeds in two distinct stages corresponding to the independent unfolding of the two domains, whereas heat denaturation proceeds in one stage, showing that the two domains behave as one cooperative unit. Recently, this folding/unfolding behavior of PGK was theoretically analyzed by Freire et al. (1992) in terms of interdomain interaction.

To achieve a structural characterization of the cold-denatured state of yeast PGK as complete as possible, we investigated the protein by combining the methods of DSC, SAXS, DLS, CD, and fluorescence.

We will show that, at 4.5 °C, the conformation of PGK resembles that of an unperturbed random coil. In accordance with the calorimetric studies, the two-stage behavior of unfolding upon cold denaturation can also be proved by structural investigations.

MATERIALS AND METHODS

Sample Preparation. Yeast 3-phosphoglycerate kinase (EC 2.7.2.3) was purchased from Boehringer Mannheim GmbH, FRG. The ammonium sulfate precipitated protein was dissolved in 20 mM sodium phosphate, pH 6.5, 10 mM EDTA, 1 mM DTT, and 0.7 M GuHCl (buffer A) and then dialyzed exhaustively against the same buffer at room temperature. The molarity of GuHCl was controlled refractometrically (Pace et al., 1989). Then the sample was applied to a FPLC-Superose 12 column (Pharmacia LKB Biotechnology). Only peak fractions were taken for the measurements. For SAXS measurements, the samples were concentrated in Centricon PM 10 microconcentrators. PGK concentrations were determined photometrically using $A_{1\text{ cm}}^{1\%} = 4.95$ at 280 nm (Adams et al., 1985). The molecular homogeneity of the protein was tested before and after the measurements in 15% sodium dodecylsulfate-polyacrylamide gels according to Laemmli (1970).

Dynamic Light Scattering. The DLS spectrometer has been described by Gast et al. (1992b). Briefly, the optical part of the spectrometer consists of an argon laser operating at $\lambda = 514.5$ nm, a thermostated cell holder, and a detection system. The latter two components are mounted on a modified X-ray goniometer, HZG4 (Freiberger Präzisionsmechanik GmbH, FRG). The homodyne autocorrelation functions, $G^2(\tau)$, are calculated by a laboratory-built 90-channel multibit multiple- τ correlator. The correlator is on-line-coupled with a PC/AT equipped with a transputer board, ALV-800 (ALV Laser Vertriebgesellschaft mbH, FRG), for fast data evaluation using the program CONTIN (Provencher, 1982a,b).

The translational diffusion coefficients, D_T , determined from the autocorrelation functions, were converted into hydrodynamic effective radii, R_S , via the Stokes-Einstein equation, $R_S = kT(6\pi\eta_0 D_T)^{-1}$, where k is Boltzmann's constant, T , the temperature in Kelvin, and η_0 , the solvent viscosity. η_0 -Values were determined in dependence on T by means of an Ubbelohde-type viscometer and a digital density meter, DMA 58 (Anton Paar K.G., Austria). All DLS measurements were made at a scattering angle of 90° using flow-through micro cells with a sample volume of 100 μ L (Hellma, FRG). The solvent and the protein solutions were filtered through either 20-nm-pore-size filters (Biotage Europe, U.K.) or 100-nm-pore-size filters (Sartorius GmbH, FRG) directly into the scattering cells.

Small-Angle X-ray Scattering. SAXS curves were measured on a SAXS-WAXS diffractometer (Freiberger Präzisionsmechanik GmbH, FRG) with slit geometry. The Cu K α radiation was collimated by five vertical slits and by Soller slits. The slit widths were adjusted in such a way that the scattering from particles with dimensions smaller than 50 nm could be collected down to the first sampling point. The methods of data processing and desmearing were previously described (Müller et al., 1986; Damaschun et al., 1991b).

Great care was taken with the extrapolation of the scattering data to 0 protein concentration. The method has been described in detail in our work on unfolded apocytochrome *c* (Damaschun et al., 1991b). Neglecting this procedure can lead to erroneous values of the compactness of the unfolded protein molecules. The reason for these errors is excluded volumes of unfolded proteins that are 1–2 orders of magnitude larger than those of the corresponding folded proteins (Damaschun et al., 1991b).

Differential Scanning Calorimetry. Scanning calorimetric measurements were performed on an MC-2D microcalorimeter (MicroCal Inc., Northampton, MA) equipped with the DA-2 data acquisition system. Baselines were recorded using buffer at varying scan rates (ranging from about 10 to 90 K/h). The baselines were adjusted for optimal cell feedback.

Protein was measured immediately after chromatography (see Sample Preparation). The thermal equilibration time before scanning was 90 min at –6 °C thermostat setting. Protein concentration was 2.2–2.5 g/L. Data was treated using the DA-2 and Fourier transform DSC software packages (Micro Cal). For the scan-rate dependence of the thermal transitions, the peak maximum obtained from the Fourier-transformed transition curve was taken, to the first approximation, as the transition temperature.

Circular Dichroism. CD measurements were performed on a J-720 spectrometer (JASCO, Japan) in 10-mm (350–250 nm) or 1-mm cells (250–200 nm) at protein concentrations of about 2 or 0.3 g/L, respectively. Mean residue ellipticities were calculated using a value of 107.4 for the mean residue weight of PGK. The spectrometer was calibrated with (+)-10-camphorsulfonic acid at 290.5 and 192.5 nm (Johnson, 1990).

Fluorescence. Fluorescence spectra were measured on an MK2 spectrometer (Farrand) at excitation wavelengths of 280 and 295 nm and protein concentrations of 0.08 g/L.

RESULTS

Dynamic Light Scattering. To check for the influence of 0.7 M GuHCl on the hydrodynamic effective dimensions of PGK, we determined the Stokes radius in the absence of GuHCl. We obtained the translational diffusion coefficient $D_{20,w}^0 = (7.21 \pm 0.05) \times 10^{-7} \text{ cm}^2 \text{ s}^{-1}$ and the corresponding Stokes radius $R_S = 2.97 \pm 0.02 \text{ nm}$. The weak concentration dependence of D can be expressed as $D_{20,w} = D_{20,w}^0 [1 + (7.8 \times 10^{-4})c]$, where c is the protein concentration in g/L. Combining our value of $D_{20,w}^0$ with the sedimentation constant $s_{20,w}^0 = 3.3 \text{ S}$ and the apparent partial specific volume $\bar{v} = 0.748 \text{ mL/g}$ taken from Roustian et al. (1980) results in the molar mass $M_{s,D} = 44\,300 \text{ g/mol}$, in excellent agreement with the chemical molar mass $M = 44\,570 \text{ g/mol}$ of yeast PGK.

In the presence of 0.7 M GuHCl, we found a small but significant increase of the Stokes radius. We determined a value of $R_S = 3.10 \pm 0.05 \text{ nm}$ at 30 °C, the temperature of maximum stability of PGK under these conditions (Griko et al., 1989).

Decreasing the temperature stepwise from 30 to 1 °C leads to a considerable increase of the Stokes radius to a value

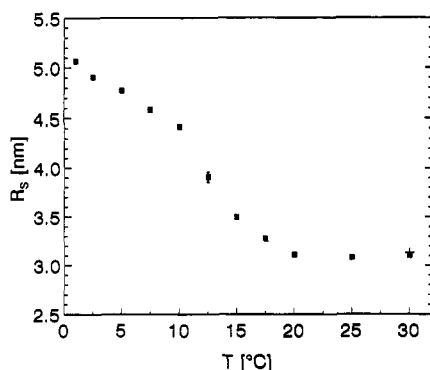


FIGURE 1: Stokes radius, R_s , of PGK in buffer A as a function of temperature. Protein concentration: 0.97 g/L. (+) R_s after refolding at 30 °C.

greater than 5 nm at 1 °C (Figure 1). As can be clearly seen, the changes in R_s proceed in two stages. The first and the second step begin at about 20 and 7.5 °C, respectively. The second transition is not yet complete at 1 °C. For technical reasons, however, measurements below 1 °C are unfeasible with our DLS spectrometer. It is noteworthy that the rates of unfolding and refolding of the protein upon decreasing and increasing temperature, and therefore the changes in R_s , are very slow. Special care was given to this fact in our experiments. The values of R_s in Figure 1 are equilibrium values. The kinetic aspects of this work are discussed in an accompanying paper (Gast et al., 1993).

The unfolding of PGK upon cold denaturation was found to be essentially reversible. Refolding by incubation at 30 °C over a period of several hours gave values of R_s only slightly larger than before cold denaturation (Figure 1).

Experiments also to measure the Stokes radii of heat-denatured PGK proved to be unsuccessful, because the protein aggregated irreversibly at temperatures above 35 °C. This was clearly indicated by a strong irreversible increase of the total scattered intensity. Contrary to this, cold denaturation did not induce any perceptible aggregation. After PGK was cooled from 30 to 1 °C and heated to 30 °C, the total scattering intensity was the same as at the beginning of the experiments.

To compare the dimensions of the cold-denatured PGK with those of the protein unfolded in GuHCl, we determined R_s in the presence of 2 M GuHCl at 20 °C. This molarity of GuHCl is sufficient to attain complete unfolding, at least according to CD criteria (Adams et al., 1985; R. Misselwitz, unpublished results). We obtained a value of $R_s = 5.66$ nm.

Small-Angle X-ray Scattering. X-ray scattering from PGK solutions (see Materials and Methods) was measured at concentrations between 3 and 8 g/L at temperatures of 28, 7, and 4.5 °C. The scattering data were desmeared and extrapolated to 0 protein concentration. Distance distribution functions were calculated from the scattering curves by Fourier transformation.

Figure 2 shows the scattering curves of PGK at 28 and 4.5 °C in the form of a Kratky plot, $i(s) \cdot s^2$ versus s , since the drastic difference between the curves can be illustrated much better by such a plot than by the conventional plot of i versus s . Guinier plots of the inner parts of both scattering curves are shown in Figure 3. The respective radii of gyration were determined according to the Guinier approximation of the scattering curves by a least-squares method. The values at 28 and 4.5 °C obtained in this manner are in perfect agreement with those calculated from the distance distribution functions.

The persistence length, a , of the unfolded protein chain at 4.5 °C can be determined directly from the Kratky plot of the scattering curve (Figure 2). The inner part of the scattering

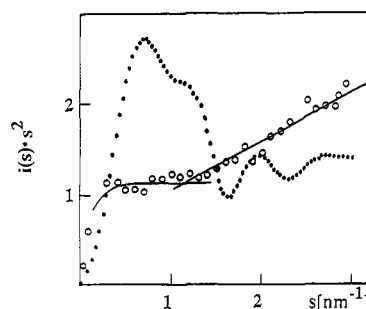


FIGURE 2: Kratky plots of the scattering data for PGK at 28 (●) and 4.5 °C (○): $i(s)$, scattered intensity; $s = 4\pi\lambda^{-1} \sin \theta$, scattering coordinate; λ , wavelength; 2θ , scattering angle. The left solid line is the fitted scattering curve of a Gaussian coil in the Debye approximation; the right solid line is the fitted scattering curve of a needle. The point of intersection of the two curves is at $s = 1.12 \text{ nm}^{-1}$ and allows us to determine the persistence length, a , of the unfolded PGK (see text).

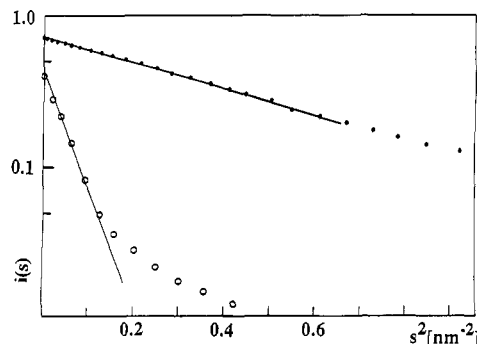


FIGURE 3: Guinier plots of the scattering curves for PGK at 28 (●) and 4.5 °C (○). The solid lines are the Guinier approximations of the inner parts of the scattering curves. The plots have been arbitrarily shifted along the ordinate for clearer presentation.

curve ($s < 1.12 \text{ nm}^{-1}$) can be approximated by the Debye scattering function of a Gaussian coil (Debye, 1947). At large angles ($s > 1.12 \text{ nm}^{-1}$), the molecule exhibits the scattering behavior of a rigid rod (needle), i.e., proportional to s^{-1} . The point of intersection of the two approximated curves yields directly the persistence length via the relation $a = 1.91/1.12 = 1.74 \text{ nm}$ (Kirste & Overthür, 1982).

We have calculated the scattering curve of the PGK molecule in aqueous solution from the atomic coordinates of crystalline PGK according to the method of Müller et al. (1990). The atomic coordinates, deposited as entry 3PGK (Watson et al., 1982), were taken from the Protein Data Bank (Bernstein et al., 1977). The shape of the calculated scattering curve coincides with the experimental curve of PGK at 28 °C for $s < 3.2 \text{ nm}^{-1}$. From the resulting scattering curve, we have determined the radius of gyration, R_G , and the largest diameter, L .

All SAXS data and related DLS data are summarized in Table I.

Differential Scanning Calorimetry. As originally reported by Privalov and co-workers (Griko et al., 1989), PGK exhibits in the presence of GuHCl a characteristic melting pattern showing both cold and heat denaturation of the protein (Figure 4). The thermogram is composed of two partly resolved peaks at about 8 and 21 °C, respectively, which correspond to cold denaturation. Thermal denaturation proceeds in a sharp transition at about 40 °C. In the present work, the transition temperature, $T_{\text{tr}} = 40.8 \pm 0.3 \text{ °C}$, enthalpy change, $\Delta H = 570 \pm 25 \text{ kJ mol}^{-1}$, and heat capacity change, $\Delta C_p = 36 \pm 9 \text{ kJ K}^{-1} \text{ mol}^{-1}$ (mean of four measurements) were found in fair agreement with former data, $\Delta H = 586 \text{ kJ mol}^{-1}$ (Griko et al., 1989) and $\Delta C_p = 31 \text{ kJ K}^{-1} \text{ mol}^{-1}$ (Freire et al., 1992).

Table I: Molecular Parameters for Yeast PGK from SAXS and DLS Measurements

temp (°C)	radius of gyration, R_G (nm)	max intraparticle distance, L (nm)	persistence length, a (nm)	Stokes radius, R_S (nm)	$\rho = R_G/R_S$
28	2.44 ± 0.01	7.8		3.09 ± 0.05	0.79 ± 0.02
7.0	7.14 ± 0.15	>20		4.64 ± 0.15	1.54 ± 0.07
4.5	7.8 ± 0.1	>24	1.74 ± 0.15	4.80 ± 0.10	1.63 ± 0.06
crystalline PGK ^a	2.48	7.94		2.91	0.85

^a Calculated from the atomic coordinates of entry 3PGK in the Protein Data Bank according to Müller et al. (1990, 1992).

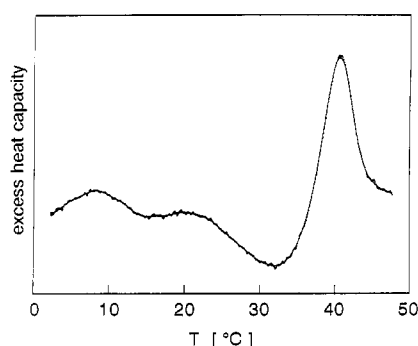


FIGURE 4: Scanning calorimetric curves of PGK in buffer A: scan rate, 1.132 K min⁻¹; protein concentration, 2.2 g/L; points, raw data; solid line, FTDSC curve.

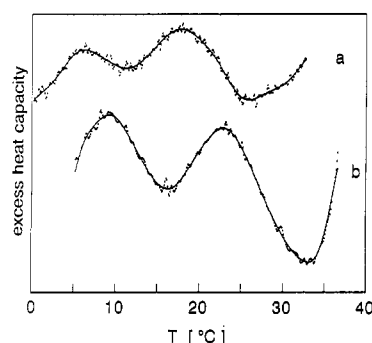


FIGURE 5: The low-temperature transitions of PGK at a scan rate of 0.241 (a) and 1.686 K/min (b). Points, raw data; solid lines, FTDSC curves.

The irreversible thermal transition was found to be scan rate dependent (Galisteo et al., 1991). The transition was analyzed for cooperativity arising from interacting domains (Brandts et al., 1989; Galisteo et al., 1991; Freire et al., 1992).

In contrast to the thermal transition at about 40 °C, cold denaturation of PGK is reversible as judged by reheating (data not shown). However, the two transitions are strongly scan rate dependent (Figure 5). The maximum position of the two cold denaturation peaks versus scan rate, varying from about 10 to 90 K h⁻¹, is shown in Figure 6. The peak maximum temperatures, linearly extrapolated to 0 scan rate, amount to $T_1^0 = 6.3 \pm 0.3$ °C and $T_2^0 = 16.5 \pm 0.5$ °C, respectively. The increase of peak maximum temperature with the scan rate is probably due to kinetic effects in slow refolding of the protein which is in the cold-denatured state before starting the scan.

Circular Dichroism. CD measurements were performed in the spectral regions of both the peptide and the aromatic chromophores at different temperatures between 30 and 1 °C. Representative CD spectra are shown in Figure 7. To ensure that the protein conformation had reached the equilibrium state after a change in temperature, we carried out time scans of the ellipticity at fixed wavelengths of 220 or 278 nm for about 2 h in each case before measuring the spectra. By way of comparison, we show additionally the CD spectra of PGK in the absence of GuHCl and in the presence

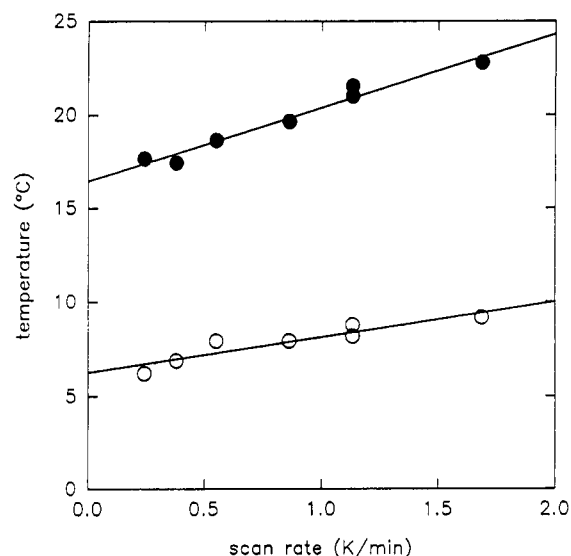


FIGURE 6: PGK low-temperature transitions: peak maximum temperature versus scan rate.

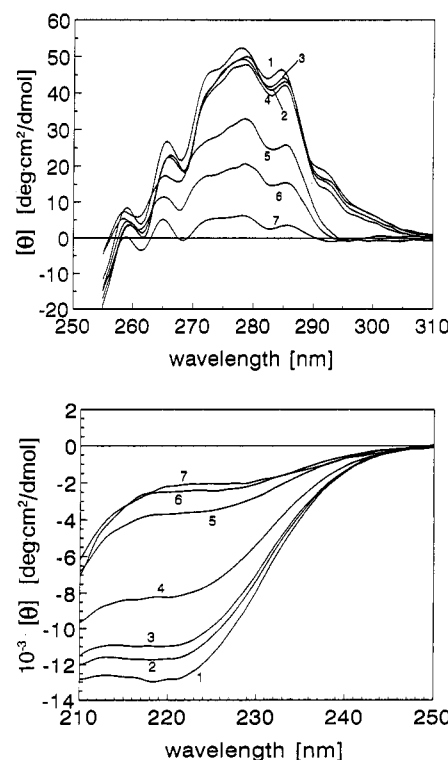


FIGURE 7: Near-ultraviolet (a, top) and far-ultraviolet CD spectra of PGK (b, bottom): (1), buffer A without GuHCl 20 °C; (2), buffer A 30 °C; (3), buffer A, 20 °C; (4), buffer A, 15 °C; (5), buffer A, 5 °C; (6), buffer A, 1 °C; (7), buffer A plus 2M GuHCl, 20 °C.

of 2 M GuHCl at 20 °C. Comparing the spectra of PGK in the absence of GuHCl with those in the presence of 0.7 M GuHCl at 30 °C, one sees that the conformation of the protein is slightly changed by this concentration of the denaturant.

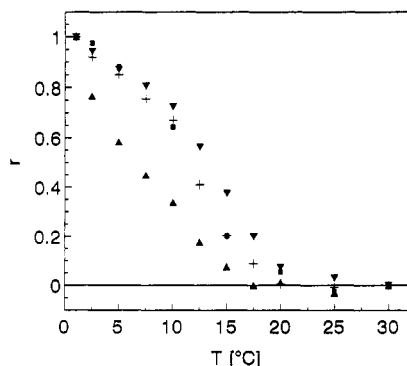


FIGURE 8: Relative changes between 30 and 1 °C upon decreasing temperature for PGK in buffer A of the mean residue ellipticity $[\theta]$ at $\lambda = 220$ nm (▼), the mean residue ellipticity $[\theta]$ at $\lambda = 278$ nm (▲), the ratio of fluorescence intensities $I(370 \text{ nm})/I(330 \text{ nm})$ (■), and the Stokes radius, R_S (+).

Particularly, some loss of regular secondary structure is indicated.

Figure 8 shows the relative changes in the mean residue ellipticities $[\theta]$ at 220 and 278 nm depending on temperature. Relative changes, r , were calculated from $r = ([\theta]_{30^\circ\text{C}} - [\theta]_{T^\circ\text{C}}) / ([\theta]_{30^\circ\text{C}} - [\theta]_{1^\circ\text{C}})$. Only minor changes of $[\theta]_{220}$ occur between 30 and 20 °C. The subsequent unfolding of the protein between 20 and 1 °C proceeds in two stages, the second one beginning at about 7.5 °C. The value of $[\theta]_{220}$ at 1 °C is very similar to that of PGK in 2 M GuHCl (see also spectra 6 and 7 in Figure 7b), indicating that little if any regular secondary structure is left at 1 °C.

The CD of the aromatic amino acids is nearly constant in the temperature range from 30 to 15 °C (see Figures 7a and 8). Below 15 °C, the ellipticity values are decreasing, with the most prominent change of $[\theta]_{278}$ between about 7.5 and 1 °C.

This differing behavior of $[\theta]_{220}$ and $[\theta]_{278}$ depending on temperature has already been described and interpreted by Griko et al. (1989). They concluded that the two domains of the PGK molecule unfold non-cooperatively on cold denaturation over different temperature ranges, because $[\theta]_{278}$ is mainly determined by the two tryptophans in the C-terminal domain, whereas changes in $[\theta]_{220}$ reflect conformational changes of the entire molecule. Therefore, the C-terminal domain must be more stable against cold denaturation than the N-terminal domain.

Comparing the CD spectra of the aromatic amino acids of PGK in buffer A at 1 °C and in 2 M GuHCl at 20 °C (Figure 7a), one sees that there is still a significant difference in the ellipticities, indicating different interactions of the aromatic side chains with their environment and/or among each other under the different conditions.

Fluorescence. The fluorescence measurements were performed at different temperatures at the excitation wavelengths $\lambda = 295$ nm for selectively exciting the tryptophans and $\lambda = 280$ nm. The protein concentration was 0.08 g/L. The maximum position of the fluorescence spectrum exhibits a red-shift from about 335 to 348 nm upon a temperature decrease from 30 to 1 °C. A similar shift has been found for the GuHCl-induced unfolding of PGK (Missiakas et al., 1990). According to the classification scheme of Burstein et al. (1973), emission maxima of proteins at about 350 nm are characteristic of solvent-accessible tryptophans. At full accessibility, however, the emission maximum is shifted to about 355 nm.

Figure 8 shows the relative changes, r , of the emission intensity ratio, $I(370 \text{ nm})/I(330 \text{ nm})$, at 295-nm excitation depending on temperature. The changes of the intensity ratio were found to be independent of the excitation wavelength;

therefore, the data for excitation at 280 nm are not shown. The most prominent increase in this ratio occurred between about 17 and 7 °C. Below and above these temperatures, only minor changes were measured, and the intensity ratio was nearly constant between 22 and 30 °C. These results are in qualitative agreement with the fluorescence data of Griko et al. (1989).

DISCUSSION

Conformation of Yeast PGK in the Presence of 0.7 M GuHCl. According to the prediction, cold denaturation of proteins in pure aqueous solution should occur below the freezing point of water (Privalov, 1990). There are two possibilities for observing cold denaturation experimentally. Either one has to work with supercooled solutions or one must choose solvent conditions where cold denaturation takes place above 0 °C. Supercooling is rather dangerous, because spontaneous freezing of the protein solution may damage the experimental device. Therefore, most experimental studies of cold denaturation have been done in appropriate solvents, decreasing the protein stability and shifting the transition of cold denaturation to more convenient temperatures above or near 0 °C.

The original work of Griko et al. (1989) on cold denaturation of yeast PGK was done under moderately destabilizing conditions. The destabilization was achieved by addition of GuHCl to the 20 mM phosphate buffer, pH 6.5. Most of their experimental data refer to the presence of 0.7 M GuHCl. In this solvent, the temperature of maximum stability of PGK is about 30 °C, and cold denaturation of the two domains occurs non-cooperatively between about 20 and 0 °C (Griko et al., 1989).

Our experiments were also performed in the presence of 0.7 M GuHCl (buffer A). It is well-known from previous CD measurements that the presence of 0.7 M GuHCl effects a decrease of the peptide chromophore ellipticity, $[\theta]_{220}$, of about 20% at 20 °C (Adams et al., 1985; Missiakas et al., 1990). This indicates some loss of regular secondary structure, i.e., mainly helix and/or β -sheet structure. Therefore, it is necessary to discuss potential differences between the conformations of PGK in pure aqueous solution and in the presence of 0.7 M GuHCl at 30 °C, the starting point of our structural investigations.

Our CD measurements (Figure 7a,b) agree with the above described previous findings. Compared to the ellipticity, $[\theta]_{220}$, of PGK in the absence of GuHCl, we found a decrease in the ellipticity values of about 10% and 15% at 30 and 20 °C, respectively, in the GuHCl-containing solvent. This results shows that even at 30 °C, the temperature of maximum stability, some elements of regular secondary structure are impaired. On the other hand, the measurements in the spectral range of the aromatic chromophores revealed only minor changes of $[\theta]_{278}$ under the influence of 0.7 M GuHCl at 30 and 20 °C compared to $[\theta]_{278}$ for PGK in the absence of GuHCl (Figure 7a). Therefore, one might assume that the rigid structure of the two domains remains essentially unchanged and that the secondary structure modification of PGK in the range from 30 to 20 °C is confined to the hinge region of the molecule, accompanied by some reorientation of the domains and, therefore, changed interdomain interactions.

The latter is corroborated by comparing the Stokes radii and the radii of gyration at 30 °C in the absence and in the presence of 0.7 M GuHCl, respectively. Without GuHCl, we determined a value of $R_S = 2.97$ nm and a frictional ratio of $f/f_{\min} = 1.26$. The frictional ratio was calculated from f/f_{\min}

$= R_S/R_{\min}$, R_{\min} being the radius of the unsolvated PGK molecule, the shape of which is assumed to be an ideal sphere. We determined $R_{\min} = (3M\bar{v}/4\pi N_A)^{1/3} = 2.36$ nm using $M = 44\,570$ g mol⁻¹ and $\bar{v} = 0.748$ cm³ g⁻¹ from Roustan et al. (1980). These authors found from sedimentation measurements a value of $f/f_{\min} = 1.27$. In the presence of 0.7 M GuHCl, we obtained at 30 °C a slightly enlarged Stokes radius $R_S = 3.09$ nm, and the frictional ratio $f/f_{\min} = 1.31$.

Our value of the radius of gyration, $R_G = 2.44$ nm, in the presence of 0.7 M GuHCl at 28 °C is also somewhat larger than those for yeast PGK in the absence of the denaturant, $R_G = 2.33$ and 2.39 nm, determined by Pickover et al. (1979) and Ptitsyn et al. (1986), respectively.

The value of $R_G = 2.48$ nm, calculated from the atomic coordinates of entry 3PGK in the Protein Data Bank, is even larger than that measured for PGK in the absence and in the presence of 0.7 M GuHCl. However, Haran et al. (1992) have recently shown by time-resolved fluorescence energy transfer measurements on site-specific labeled yeast PGK that the average interdomain distance of PGK in solution is about 0.8 nm smaller than in the crystal structure. This effect might explain the discrepancy between the experimentally determined radii of gyration and the calculated one.

All in all, our experimental data from CD, DLS, and SAXS lead to the following suggestion. The conformation of PGK is affected by the denaturant at 30 °C in such a manner that the mutual orientation of the domains changes somewhat, leading to a slight increase in the overall dimensions of the molecule. The reorientation of the domains is probably due to secondary structure changes in the hinge region. The compact structure of the domains, however, remains intact.

Cold Denaturation-Induced Unfolding of PGK Proceeds in Two Stages with Slow Kinetics. The structural changes induced by decreasing the temperature from 30 to 1 °C proceed in two stages. This is clearly indicated by the increase in the overall molecular dimensions as monitored by the dependence of the Stokes radius on temperature as well as by the temperature dependence of the ellipticity at 220 nm (Figures 1 and 8). $[\theta]_{220}$ serves to monitor global changes in the secondary structure of the protein. The first and the second stage of unfolding set in at about 20 and 7.5 °C, respectively. This two-stage behavior was to be expected because of the non-cooperative melting and renaturation of the two domains of PGK upon and after cold denaturation (Griko et al., 1989). Our DSC measurements (Figure 4) agree with these previous findings.

Comparing the changes of the CD in the spectral ranges of the peptide chromophores, $[\theta]_{220}$, and the aromatic chromophores, $[\theta]_{278}$, as well as of the fluorescence intensity ratio, $I(370\text{ nm})/I(330\text{ nm})$, depending on decreasing temperature (Figure 8), one sees that these changes proceed nonsimultaneously. The changes of $[\theta]_{220}$, monitoring changes of secondary structure of the entire molecule, set in at higher temperatures than those of the fluorescence intensity ratio and particularly of $[\theta]_{278}$. The latter changes are primarily due to changes in the environment of the two tryptophan residues, which are both located in the C-terminal domain. One can conclude, therefore, that the N-terminal domain unfolds prior to the C-terminal domain during cold denaturation, as has already been pointed out by Griko et al. (1989). This conclusion is also in agreement with investigations of the GuHCl-induced unfolding of yeast PGK by Adams et al. (1985). They found that the domains have different free energies of stabilization, the C-terminal domain being the more stable one.

It should be emphasized that the structural changes after a change in temperature are governed by very slow kinetics

(Gast et al., 1992b). This is impressively demonstrated by the dependence of the DSC measurements on the scan rate (Figures 5 and 6). Neglect of this fact may lead to erroneous results and to distorted dependences of the respective quantities on temperature. The measurements of the dependence on temperature of the structural parameters (Figures 1, 7, and 8) were very time-consuming for this reason. Mostly, we performed at first time scans of the parameter after changing the temperature, to be sure that the final equilibrium value had been reached. The kinetic aspects are discussed in detail in an accompanying paper (Gast, et al., 1993).

The reversibility of the cold denaturation-induced structural changes was tested on the basis of the Stokes radius and the CD spectra in both the far- and the near-ultraviolet region. After the measurements at the lowest temperature, the samples were incubated at 30 °C for some hours until equilibrium was reached again. We found complete reversibility of the CD spectrum in the near-ultraviolet region, whereas the Stokes radius was always a little larger than the initial value (Figure 1). The CD spectrum in the far-ultraviolet region was not fully reversible, either. After the temperature cycle 30 °C → 1 °C → 30 °C, there remained a loss of about 10% of $[\theta]_{220}$ compared to the initial ellipticity at 30 °C. These findings lead to the conclusion that the domains refold correctly but that their mutual arrangement does not regain its initial state, probably due to some remaining changes in the structure of the hinge region.

Conformation of PGK in the Cold-Denatured State. The SAXS curve for cold-denatured PGK (Figure 2) shows the behavior typical of the scattering curve of a coiled-chain molecule (see Figure 3 in Kratky, 1982; Kirste & Oberthür, 1982). At first, the scattered intensity, i , is proportional to s^{-2} . This part of the scattering curve is followed by a range where $i \propto s^{-1}$ (Figure 2). From the point of intersection of both scattering curve sections, we obtain the persistence length $a = 1.74$ nm and the corresponding length of the statistical chain segment $b = 3.48$ nm. The persistence length and the statistical chain segment are equivalent to segments of 5 and 10 amino acids of the chain contour, respectively. The calculated contour length of the extended PGK chain amounts to $L = 143$ nm. The value of the persistence length for cold-denatured PGK of $a = 1.74$ nm is only slightly smaller than the value of $a = 1.81$ nm that was determined by the same method for acid-denatured apocytochrome *c* (Damaschun et al., 1991b).

The radius of gyration, R_G , was found to be $R_G = 7.8$ nm at 4.5 °C (Table I; Figure 3). The expansion of the molecular volume caused by cold denaturation can be assessed by $q_{\text{vol}} = R_{G,4.5^\circ\text{C}}^3/R_{G,28^\circ\text{C}}^3$ to be $q = 33$, meaning that the chain takes up a 30-fold larger volume when unfolded by cold denaturation than the volume of the folded polypeptide chain in the native state. It should be emphasized that the expansion of the "hydrodynamic" volume, calculated from the ratio of the cubes of the Stokes radii, R_S , is much smaller than the "geometric" volume expansion, namely, only 3.7.

This is due to the strong dependence of the so-called ρ -factor, $\rho = R_G/R_S^1$, on the conformation of the molecules under investigation. The ρ -value for folded PGK at 28 °C is $\rho = 0.79$, this value being typical for folded globular proteins. The mean value for all single-chain, compactly folded globular proteins, the crystal structures of which are included in the Protein Data Bank (Bernstein et al., 1977), amounts to $\rho = 0.80 \pm 5\%$ SD (Damaschun et al., 1993).

We obtained $\rho = 1.63 \pm 0.06$ for cold-denatured PGK molecules (Table I). Such a ρ -value is also characteristic of strongly aspherical compact particles, e.g., of a prolate ellipsoid of rotation with an axial ratio of 20:1. However, the scattering

curve for such an elongated ellipsoid does not agree with the experimental curve. Tanford (1961) has derived the ρ -factor for a Gaussian coil. He obtained the value $\rho = 1.51$. We have determined experimentally a slightly greater value of $\rho = 1.55$ for acid-denatured apocytochrome *c* (Damaschun et al., 1991a,b). In addition to the shape of the scattering curve, the value $\rho = 1.63 \pm 0.06$, obtained by us for PGK, is further evidence of the random-coil structure of PGK at temperatures lower than 4.5 °C. However, this conclusion has to be qualified as follows.

Benoit and Doty (1953) have derived the equation

$$\langle R_G^2 \rangle = \frac{La}{3} \left[1 - \frac{3a}{L} + \frac{6a^2}{L^2} - \frac{6a^3}{L^3} + \frac{6a^3 e^{-L/a}}{L^3} \right]$$

relating the radius of gyration, R_G , to the contour length, L , and the persistence length, a , of a random chain obeying persistence statistics. If we calculate the expectancy value of R_G from this equation using the experimental persistence length, a , and the theoretical contour length, L , we obtain $R_G = 8.94$ nm. This value is significantly larger than the value $R_G = 7.8$ nm that was determined experimentally at 4.5 °C. To reach agreement between the values obtained from the Benoit-Doty equation and from SAXS measurements, we must assume that the contour length of the investigated molecule is 24% shorter than the length of an extended chain consisting of 415 amino acids in β -strand conformation. In other words, the polypeptide chain is partially contracted, e.g., by fluctuating α -helical segments or small collapsed regions. This conclusion is in full agreement with the CD spectra (Figure 7). The spectra also indicate a content of remaining structure in the form of helical segments or small folded regions. If we calculate the shortening of the chain at 7.5 °C by the same method, we obtain a reduction of 36% compared to the extended chain.

Unfortunately, it was unfeasible for technical reasons to measure the radius of gyration directly at 1 °C. If we calculate the radius of gyration from the Stokes radius at 1 °C with $\rho = 1.63$, we obtain $R_G = 1.63R_s = 8.23$ nm. This estimation can be interpreted in such a way that the "remaining structures" disappear to a great extent below 1 °C. Really, the far-ultraviolet CD spectra coincide at these temperatures with the spectrum of the protein in 2 M GuHCl (Figure 7b). In contrast to this behavior, the near-ultraviolet spectra of the protein at 1 °C in 0.7 M GuHCl and at 20 °C in 2 M GuHCl exhibit noticeable differences (Figure 7a), pointing to different interactions of the aromatic chromophores among themselves and/or with their environment under these conditions. This might imply different distance distribution functions of the aromatic amino acids with some nonrandomness in the case of the cold-denatured protein. However, this is only of minor influence on the distance distribution function averaged over all amino acid pairs. The low-temperature SAXS curve, being the Fourier transformation of this distance distribution, can be described by random persistence statistics (see above).

But it should be remarked that the scattering curve (Figure 2) exhibits weakly developed oscillations around both the Debye and the needle scattering function. These oscillations indicate that there also exists a persistence of curvature in addition to the persistence of direction. We assume the following reason for the persistence of curvature. The ϕ, ψ -angles corresponding to a right-handed α -helix are energetically more favorable than the angles corresponding to a left-handed helix for all amino acids except glycine and will, therefore, occur more frequently in the unfolded state than the latter.

The internal organization of a protein is determined by local and nonlocal interactions of the chain segments and by interactions of the chain segments with the solvent and its components (Chan & Dill, 1991). Under special solvent conditions, referred to as the Flory θ state (Flory 1969), the nonlocal interactions are negligible, and the configurational states of polypeptides are governed primarily by local interactions. Theoretical calculations and experimental data from hydrodynamic and scattering methods have shown that the dimensions of the unfolded polypeptide chain of an "average" globular protein at quasi- θ conditions can be estimated from the relation

$$\langle R_G^2 \rangle = (0.9 \pm 0.1)n_A/6 \text{ nm}^2$$

where n_A is the number of amino acids in the chain (Miller & Goebel, 1968; Damaschun et al., 1991b; Bohdanecky & Petrus, 1991). Provided that the attractive nonlocal interactions are compensated by repulsive ones on average, we would expect for the radius of gyration of the unfolded PGK chain a value of $R_{G,\theta} = 7.88 \pm 0.5$ nm. According to Flory (1969), the unperturbed and the perturbed chain are related through

$$\langle R_G^2 \rangle = \alpha^2 \langle R_{G,\theta}^2 \rangle$$

If attractive interactions predominate, i.e., if the chain is partially in compact conformation, then $\alpha < 1$; if repulsive interactions predominate, then $\alpha > 1$.

We determined from our data a value of $\alpha = 1.04$ for the polypeptide chain of PGK at 1 °C. This value decreases to $\alpha = 0.31$ when the temperature is increased to 28 °C.

Unfortunately, it was impossible to determine the radius of gyration for heat-denatured PGK, because the protein aggregated at temperatures above 35 °C. However, we can refer to data for heat-denatured streptokinase (Damaschun et al., 1992; Gast et al., 1992a). Streptokinase is also a single-chain protein without disulfide bridges and consists of 414 amino acids, i.e., its n_A is nearly the same as the n_A of PGK. The radius of gyration of heat-denatured streptokinase was determined to be $R_G = 6.7$ nm, $\alpha = 0.85$ (H. Damaschun, unpublished results). The radii of gyration of PGK and streptokinase, unfolded in GuHCl, amount to $R_G = 8.77$ nm, $\alpha = 1.11$, and $R_G = 8.58$ nm, $\alpha = 1.09$, respectively. The radii of gyration of both proteins in GuHCl were calculated from the Stokes radii with $\rho = 1.55$. Thus we see that for these proteins the radius of gyration of the cold-denatured protein is larger than that of the heat-denatured protein but smaller than that of the protein unfolded in GuHCl. This result is in agreement with the prediction by Dill et al. (1989) based on the heteropolymer model.

Conclusions. (i) In the presence of 0.7 M GuHCl at 30 °C, PGK is a compactly folded molecule. At a resolution of 1 nm, its kidney-like shape is very similar to that in the crystalline state. (ii) The two domains unfold non-cooperatively upon cooling, i.e., first the N-terminal domain, and then the C-terminal domain, unfolds. The DSC peak maxima of the excess heat capacity, extrapolated to 0 scan rate, are positioned at 16.5 and 6.3 °C, respectively. The temperature-dependent structural parameters indicate that unfolding of the N-terminal domain sets in at 20 °C. The unfolding of the C-terminal domain begins at about 8 °C. (iii) At both 4 and 1 °C in the presence of 0.7 M GuHCl, the PGK molecule exhibits the behavior typical of a chain molecule in random-coil conformation. The geometrical molecular volume is 30 times larger than that of PGK in the native state. The molecular dimensions nearly correspond to the expectancy value for a Gaussian coil of a polypeptide chain consisting of 415 amino acids under

θ -like conditions.

On the basis of the physical characterization of PGK in both the folded and the unfolded state, we have investigated the kinetics of unfolding and refolding by DLS and CD methods. These studies were made feasible by applying rather simple T-jump techniques, because time constants of the order of several minutes in magnitude are characteristic of the unfolding/refolding process in the GuHCl-containing solvent (Gast et al., 1992b). The results of the kinetic measurements are described in a separate paper (Gast et al., 1993).

ACKNOWLEDGMENT

The authors wish to thank Mr. R. Kröber for skillful help with the experiments and Mrs. D. Otto for the careful processing of the manuscript.

REFERENCES

- Adams, B., Burgess, R. J., & Pain, R. H. (1985) *Eur. J. Biochem.* 152, 715–720.
- Antonino, L. C., Kautz, R. A., Nakano, T., Fox, R. O., & Fink, A. L. (1991) *Proc. Natl. Acad. Sci. U.S.A.* 88, 7715–7718.
- Azuaga, A. J., Galisteo, M. L., Mayorga, O. L., Cortijo, M., & Mateo, P. L. (1992) *FEBS Lett.* 309, 258–260.
- Banks, R. D., Blake, C. C. F., Evans, P. R., Haser, R., Rice, D. W., Hardy, G. W., Merrett, M., & Phillips, A. W. (1979) *Nature* 279, 773–777.
- Benoit, H., & Doty, P. (1953) *J. Phys. Chem.* 57, 958–963.
- Bernstein, F. C., Koetzle, T. F., Williams, G. J. B., Meyer, E. F., Jr., Brice, M. D., Rodgers, J. R., Kennard, O., Shimanouchi, T., & Tasumi, M. (1977) *J. Mol. Biol.* 112, 535–542.
- Bohdanecky, M., & Petrus, V. (1991) *Int. J. Biol. Macromol.* 13, 231–234.
- Brandts, J. F. (1964) *J. Am. Chem. Soc.* 86, 4291–4301.
- Brandts, J. F., Hu, C. Q., Lin, L.-N., & Mas, M. T. (1989) *Biochemistry* 28, 8588–8596.
- Burstein, E. A., Vedenkina, N. S., & Ivkova, M. N. (1973) *Photochem. Photobiol.* 28, 263–279.
- Chan, H. S., & Dill, K. A. (1991) *Annu. Rev. Biophys. Biophys. Chem.* 20, 447–490.
- Chen, B., & Schellman, J. A. (1989) *Biochemistry* 28, 685–691.
- Chen, B., Baase, W. A., & Schellman, J. A. (1989) *Biochemistry* 28, 691–699.
- Damaschun, G., Gernat, Ch., Damaschun, H., Bychkova, V. E., & Ptitsyn, O. B. (1986) *Int. J. Biol. Macromol.* 8, 226–230.
- Damaschun, G., Damaschun, H., Gast, K., Zirwer, D., & Bychkova, V. E. (1991a) *Int. J. Biol. Macromol.* 13, 217–221.
- Damaschun, G., Damaschun, H., Gast, K., Gernat, Ch., & Zirwer, D. (1991b) *Biochim. Biophys. Acta* 1078, 289–295.
- Damaschun, G., Damaschun, H., Gast, K., Gerlach, D., Misselwitz, R., Welfle, H., & Zirwer, D. (1992) *Eur. Biophys. J.* 20, 355–361.
- Damaschun, G., Damaschun, H., Gast, K., Misselwitz, R., Zirwer, D., Gührs, K.-H., Hartmann, M., Schlott, B., Triebel, H., & Behnke, D. (1993) *Biochim. Biophys. Acta* 1161, 244–248.
- Debye, P. (1947) *J. Phys. Colloid Chem.* 51, 18–32.
- Dill, K. A., & Shortle, D. (1991) *Annu. Rev. Biochem.* 60, 795–825.
- Dill, K. A., Alonso, D. O. V., & Hutchinson, K. (1989) *Biochemistry* 28, 5439–5449.
- Flory, P. J. (1969) *Statistical Mechanics of Chain Molecules*, John Wiley & Sons, New York.
- Freire, E., Murphy, K. P., Sanchez-Ruiz, J. M., Galisteo, M. L., & Privalov, P. L. (1992) *Biochemistry* 31, 250–256.
- Galisteo, M. L., Mateo, P. L., & Sanchez-Ruiz, J. M. (1991) *Biochemistry* 30, 2061–2066.
- Gast, K., Damaschun, G., Damaschun, H., Misselwitz, R., Zirwer, D., & Bychkova, V. A. (1992a) in *Laser Light Scattering in Biochemistry* (Harding, S. E., Sattelle, D. B., & Bloomfield, V. A., Eds.) pp 209–224, The Royal Society of Chemistry, Thomas Graham House, Cambridge.
- Gast, K., Damaschun, G., Misselwitz, R., & Zirwer, D. (1992b) *Eur. Biophys. J.* 21, 357–362.
- Gast, K., Damaschun, G., Damaschun, H., Misselwitz, R., & Zirwer, D. (1993) *Biochemistry* (following article in this issue).
- Griko, Yu. V., Venyaminov, S. Yu., & Privalov, P. L. (1989) *FEBS Lett.* 244, 276–278.
- Haran, G., Haas, E., Szpikowska, B. K., & Mas, M. T. (1992) *Proc. Natl. Acad. Sci. U.S.A.* 89, 11764–11768.
- Harlos, K., Vas, M., & Blake, C. F. (1992) *Proteins: Struct., Funct., Genet.* 12, 133–144.
- Hu, C. Q., & Sturtevant, J. M. (1987) *Biochemistry* 26, 178–182.
- Jaenicke, R. (1987) *Prog. Biophys. Mol. Biol.* 49, 117–237.
- Johnson, W. C., Jr., (1990) *Proteins: Struct., Funct., Genet.* 7, 205–214.
- Kirste, R. G., & Overthür, R. C. (1982) in *Small-angle X-ray scattering* (Glatter, O., & Kratky, O., Eds.) pp 387–431, Academic Press, London.
- Kratky, O. (1982) in *Small-angle X-ray scattering* (Glatter, O., & Kratky, O., Eds.) pp 361–386, Academic Press, London.
- Kuroda, Y., Kidokoro, S., & Wada, A. (1992) *J. Mol. Biol.* 223, 1139–1153.
- Kuwajima, K. (1989) *Proteins: Struct., Funct., Genet.* 6, 87–103.
- Laemmli, U. K. (1970) *Nature* 227, 680–685.
- Miller, W. G., & Goebel, C. V. (1968) *Biochemistry* 7, 3925–3935.
- Missiakas, D., Betton, J.-M., Minard, P., & Yon, J. M. (1990) *Biochemistry* 29, 8683–8689.
- Müller, J. J., Zalkova, T. N., Damaschun, G., Misselwitz, R., Serdyuk, I. N., & Welfle, H. (1986) *Stud. Biophys.* 112, 151–162.
- Müller, J. J., Damaschun, G., & Schrauber, H. (1990) *J. Appl. Crystallogr.* 23, 26–34.
- Müller, J. J., Pankow, H., Poppe, B., & Damaschun, G. (1992) *J. Appl. Crystallogr.* 25, 803–806.
- Nojima, H., Ikai, A., Oshima, T., & Noda, H. (1977) *J. Mol. Biol.* 116, 429–442.
- Pace, C. N., & Tanford, C. (1968) *Biochemistry* 7, 198–208.
- Pace, C. N., Shirley, B. A., & Thomson, J. A. (1989) in *Protein structure. A practical approach* (Creighton, T. E., Ed.) pp 311–330, IRL Press, Oxford.
- Pickover, C. A., McKay, D. B., Engelman, D. M., & Steitz, T. A. (1979) *J. Biol. Chem.* 254, 11323–11329.
- Privalov, P. L. (1990) *Critical Rev. Biochem. Mol. Biol.* 25, 281–305.
- Privalov, P. L., & Gill, S. J. (1988) *Adv. Protein Chem.* 39, 191–234.
- Provencher, S. W. (1982a) *Comput. Phys. Commun.* 27, 213–227.
- Provencher, S. W. (1982b) *Comput. Phys. Commun.* 27, 229–242.
- Ptitsyn, O. B. (1987) *J. Protein Chem.* 6, 273–293.
- Ptitsyn, O. B., Pavlov, M. Yu., Sinev, M. A., & Timchenko, A. A. (1986) in *Multidomain Proteins* (Patthy, L., & Friedrich, P., Eds.) pp 9–25, Akademiai Kiado, Budapest.
- Roustan, C., Fattoum, A., Jeanneau, R., & Pradel, L. (1980) *Biochemistry* 19, 5168–5175.
- Sosnick, T. R., & Trewhella, J. (1992) *Biochemistry* 31, 8329–8335.
- Tamura, A., Kimura, K., Takahara, H., & Akasaka, K. (1991a) *Biochemistry* 30, 11307–11313.
- Tamura, A., Kimura, K., & Akasaka, K. (1991b) *Biochemistry* 30, 11313–11320.
- Tanford, C. (1961) *Physical Chemistry of Macromolecules*, pp 336–346, John Wiley & Sons, New York.
- Tanford, C. (1968) *Adv. Protein Chem.* 23, 121–282.
- Watson, H. C., Walker, N. P. C., Shaw, P. J., Bryant, T. N., Wendell, P. L., Fothergill, L. A., Perkins, R. E., Conroy, S. C., Dobson, M. J., Tuite, M. F., Kingsman, A. J., & Kingsman, S. M. (1982) *EMBO J.* 1, 1635–1640.